processes

MDPI

Article

Nitrogen Removal from the High Nitrate Content Saline Denitration Solution of a Coal-Fired Power Plant by MFC

Shaoan Cheng *, Zhipeng Huang and Zhihua Wang

State Key Laboratory of Clean Energy Utilization, Department of Energy Engineering, Zhejiang University, Hangzhou 310027, China

* Correspondence: shaoancheng@zju.edu.cn

Abstract: Oxidation denitration is one of the most efficient ways to remove NOx from flue gas in a coal-fired power plant. However, this oxidation denitration produces saline solution containing a high concentration of nitrate, which needs to be well treated. In this paper, MFC was firstly used to treat the high nitrate content saline denitration solution from ozone oxidation denitration of a coal-fired power plant. The influences of chemical oxygen demand (COD) and initial nitrate concentration on the nitrate removal and electricity generation of MFC were investigated by sequencing batch mode. The results showed that using MFCs could efficiently remove nitrate from coal-fired power plant saline denitration solution with nitrate nitrogen (NO_3^--N) concentration up to 1510 mg/L. The average nitrate nitrogen removal rate was as high as 248.3 mg/(L·h) at initial nitrate nitrogen concentration of 745 mg/L and COD concentration of 6.5 g/L, which was eight times as high as that of the conventional biological method. Furthermore, the MFC required an average COD consumption of 3.42 g/g-NO_3^--N which was lower than most of the conventional biological methods. In addition, MFC could produce a maximum power density of 241.1 mW/m^2 while treating this saline denitration solution.

Keywords: saline denitration solution; microbial fuel cell; high nitrate; nitrate removal; electricity generation

check for updates

Citation: Cheng, S.; Huang, Z.; Wang, Z. Nitrogen Removal from the High Nitrate Content Saline Denitration Solution of a Coal-Fired Power Plant by MFC. *Processes* **2022**, *10*, 1540. https://doi.org/10.3390/pr10081540

Academic Editor: Bipro R. Dhar

Received: 23 May 2022
Accepted: 2 August 2022
Published: 5 August 2022

Publisher's Note: MDPI stays neutral with regard to jurisdictional claims in published maps and institutional affiliations.

Copyright: © 2022 by the authors. Licensee MDPI, Basel, Switzerland. This article is an open access article distributed under the terms and conditions of the Creative Commons Attribution (CC BY) license (https://creativecommons.org/licenses/by/4.0/).

1. Introduction

Nitrogen oxides (NO_X) is a major atmosphere pollutant that could cause acid rain, and photochemical smog, and contribute to particulate matter, tropospheric ozone, and global warming. Controlling the emission of NO_X is essential [1–3]. At present, most NO_X comes from the combustion of fossil fuel [4]. Coal-fired power plants contribute to over half of total NO_X emission from human activities [5,6]. Post-combustion control is usually used in the coal-fired power plant to reduce NO_X emissions to meet the emission standards [7,8].

The post-combustion control of NO_X emissions is usually conducted in dry processes or wet processes. Most of the dry processes, such as selective catalytic reduction (SCR) and selective non-catalytic reduction (SNCR), have been industrialized for removing NO_X from flue gas in a coal-fired power plant, due to their high efficiency and capability of removing multi-pollutants simultaneously [9–11]. However, the dry process still exists, and is associated with some problems like high energy consumption [12–14], easy deactivation of adsorbents/catalysts [15,16], secondary pollution [17–19], a strict temperature window and high cost [20,21]. Alternatively, the wet processes which removed NO_X in flue gas through direct absorption into the solution might avoids some problems of the dry process [22–24]. However, the efficiency of NO_X direct absorption was essentially low because of the very low solubility of nitric oxide (NO) which accounted for more than 95% of NO_X produced by coal combustion [25,26]. To improve the absorption efficiency of NO_X, several common oxidants such as sodium hypochlorite (NaClO) [27], sodium chlorite ($NaClO_2$) [28], sodium chlorate ($NaClO_3$) [29], potassium permanganate ($KMnO_4$) [30] and

ozone (O_3) [31,32] have been investigated to oxidize NO to high valence nitrogen oxides such as nitrogen dioxide (NO_2) and/or nitrogen pentoxide (N_2O_5) that have much higher solubility, forming oxidation denitration technology. Among all these oxidants, ozone had been found to be one of the most efficient and environment-friendly oxidants. It could directly oxidize NO to N_2O_5 in a gas phase at high reaction rate and high conversion efficiency, while N_2O_5 could quickly and completely dissolve into water to form nitrate solution, resulting in very high removal efficiency of NO_X from flue gas. Meanwhile, the residual ozone could be rapidly decomposed to oxygen (O_2) without secondary pollution. Therefore, the ozone oxidation technology has advantages of low temperature, no massive adjustment in operation, saving space, no secondary pollution, Nitrogen sources recovery, and potential to ultra-low emissions for flue gas pollutants treatment. In recent years, the ozone oxidation denitration technology has been gradually applied to remove NO_X from flue gas in the coal-fired power plant [33–35].

However, ozone oxidation denitration or other wet processes would produce high nitrate content saline denitration solution. If discharged directly, the high nitrate content saline denitration solution would cause water quality deterioration and seriously influence human health [36]. In order to make ozone oxidation denitration or other wet processes more attractive to the application based on the cost and sustainable development, the nitrate in saline denitration solution must be removed to allow for water reuse or environmentally-friendly discharge. Removing nitrogen from this high nitrate content saline denitration solution is usually difficult and costly by using either physicochemical methods or biological methods [37,38]. Although the biological method was used to remove nitrogen from wastewater in a cost-effectivene way [39,40], they were mostly used to efficiently treat the wastewater containing nitrate nitrogen less than 1000 mg/L [41,42]. In addition, the salinity of wastewater is another important factor affecting biological denitrification [43]. Therefore, developing technology to treat saline wastewater containing high concentration nitrate is still needed.

Microbial fuel cell (MFC) is a new biological technology that is capable of synchronously treating wastewater and recovering chemical energy contained in the wastewater [44,45]. It has been considered as the most sustainable wastewater treatment technology in which treating wastewater does not need energy input but gain energy output. In recent years, MFC has been thoroughly investigated to treat various wastewaters by removing not only the chemical oxygen demand (COD), but also other pollutants like nitrogen, sulfur and phosphate [46–48]. For nitrogen removal, MFC has shown several advantages over the traditional biological methods such as low cost resulting from the reduction in the requirement of carbon source [49] and sludge production [50], as well as good capability of treating a wide region of nitrate concentrations [51].

The objective of this study was to examine the feasibilities of removing nitrogen from high nitrate content saline denitration solution produced in the coal-fired power plant by using MFC for the first time. The influences of COD addition and initial nitrate nitrogen concentration on nitrate removal and electricity generation of MFC were investigated.

2. Materials and Methods

2.1. Characteristics of Denitration Solution

The denitration wastewater was gathered from a local coal-fired power plant where ozone oxidation denitration technology was used to remove NO_X from flue gas. The denitration solution contained 1510 ± 10 mg/L NO_3^--N, 8192 ± 20 mg/L Cl^-, 5928 ± 16 mg/L SO_4^{2-}, 4.2 ± 0.6 mg/L NO_2^--N, with an electric conductivity of 28.2 mS/cm and a pH of 6.5.

2.2. MFCs Set-Up and Inoculation

Cubic-shaped single chamber MFCs were constructed as previously reported [52]. The cathode was the air-cathode (projected surface area were 7 cm^2) prepared using activated carbon as a catalyst, polytetrafluoroethylene (PTFE) as a binder, and nickel foam as a

current connector [53]. The anode was a carbon brush (diameter of 2.5 cm and length of 2.5 cm) that horizontally placed at the center of cylindrical reactor chamber [54]. A glass bottle (volume of 15 mL) was set on the top of the reactor chambers as the reactor headspace to collect the gases produced during the operation of MFC. The top of the bottle was sealed by a rubber stopper, and a needle penetrated through the stopper to release the gas pressure of the headspace. The effective volume of MFC was 28 mL (Figure 1), the cathode and the anode were connected with a titanium wire and an external resistor of 1000 Ω.

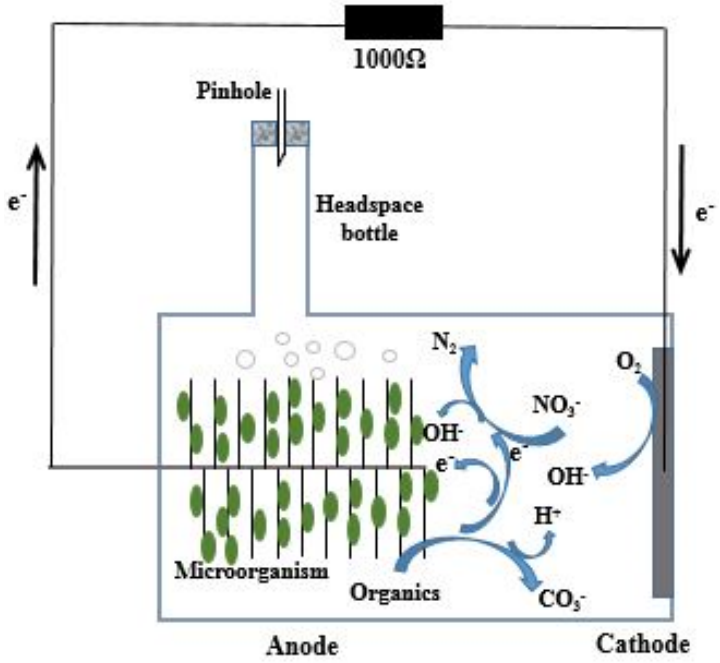


Figure 1. The schematic diagram of the microbial fuel cell reactor.

MFCs were inoculated with a mixture (1:1 in volume) of effluent and wastewater, and 1 g/L sodium acetate (NaAc) was added to the mixture during inoculation. The effluent was collected from MFC which was initially inoculated with sludge and had been operated in a fed-batch mode for more than three years, and wastewater was gathered from the nitrification tank of a local sewage treatment plant. The inoculation process was conducted for 7 cycles. Each cycle lasted 1 day, and then fresh inoculum replaced the original. After inoculation, MFCs were fed with synthetic wastewater including 200 mg/L NO_3^--N, 1.5 g/L NaAc and 50 mM PBS (pKa = 7.0; $Na_2HPO_4 \cdot 12H_2O$ 11.466 g/L; $NaH_2PO_4 \cdot 2H_2O$ 2.75 g/L; KCl 0.13 g/L; NH_4Cl 0.31 g/L). MFCs were operated for 3 months to reach stable performance for electricity generation and nitrate removal. All MFCs were operated in a fed-batch mode at a controlled temperature of 30 °C.

2.3. MFCs Operation

After start-up, the MFCs were run with saline denitration solution added with different concentrations of NaAc to vary COD concentration (5 g/L, 6.5 g/L, 9.5 g/L and 11 g/L) in order to explore the influence of COD concentration on nitrate removal. To study the influence of initial nitrate nitrogen concentration on nitrate removal, MFCs were operated with the diluted saline denitration solution at a fixed COD concentration of 6.5 g/L. The diluted saline denitration solution containing nitrate nitrogen concentrations of 1510 mg/L, 755 mg/L, 505 mg/L and 377 mg/L were obtained by diluting the raw saline denitration wastewater with mixed solution of sodium chloride (NaCl) and sodium sulfate (Na_2SO_4) to keep the same anion concentration. MFCs were also operated under open-circuit condition to compare the nitrate removal performance through the biological process with that through the bioelectrochemical process. At each experimental condition, the MFCs were operated for 6 cycles to ensure sufficient adaptation to the new environment.

All experiments were repeated three times, and results of nitrate nitrogen concentrations, nitrite nitrogen concentrations as well as output power densities were taken as the average values of three experiments, with standard deviation of less than 10%.

2.4. Analytical Methods

Concentrations of nitrate nitrogen (NO_3^--N) and nitrite nitrogen (NO_2^--N) were measured by chromic acid method and diazotization method (DR2800, HACH Company, Loveland, CO, USA) [55], respectively. The COD concentration was measured by USEPA digestion colorimetric method (DRB200 and DR2800, HACH Company, Loveland, CO, USA) [55]. The average COD consumption for nitrate removal was evaluated as the removal of COD concentration (g/L) per the removal of nitrate nitrogen concentration (g NO_3^--N/L). The electric conductivity and pH of the solution were measured by conductivity meter (LE703 IP67, Mettler Toledo, Urdorf, Switzerland) and pH meter (LE438, Mettler Toledo, Urdorf, Switzerland), respectively.

The cell voltage across the external resistor was automatically recorded using a data acquisition system (Agilent 34970A, Agilent Technologies, Palo Alto, CA, USA) every 20 min. The current was calculated by I = E/R, where E is cell voltage and R is the external resistor. The power output of MFC was calculated as P = IE. The power density curve and polarization curve was obtained by varying external resistance with operation time of 20 min at each resistor, while power density and current density were based on the cathode surface area. The anodic pH was continuously monitored by pH meter (PHSJ-5, INESA Instrument, Shanghai, China) and automatically recorded every 3 min.

The anode of MFC was taken out from the reactor, and then rinsed with deionized water, and dried. The precipitate on the anodic surface was scraped off for crystal analysis. The crystallinity of the precipitate was characterized by X-ray diffraction (XRD, Rigaku D/Max 2500), performed with a Cu Kα radiation at 40 kV and 150 mA.

3. Results and Discussion

3.1. Influence of COD Concentration on Treatment of Saline Denitration Solution

3.1.1. Influence of COD Concentration on Removal of Nitrate Nitrogen

Figure 2A showed the nitrate concentration changed as the MFC operation time increased. It can be seen that the concentrations of nitrate and COD decreased gradually as time went on, and the average removal rate of nitrate nitrogen decreased as well. From the 1st to the 3rd hour, the average removal rate of nitrate nitrogen first increased and then decreased with the increase of COD concentration, while the maximum average removal rate of nitrate nitrogen was 6.5 g/L COD and the minimum average removal rate of nitrate nitrogen was 11 g/L COD. From the 5th to the 10th hour, the average removal rate of nitrate nitrogen of MFCs with 11 g/L COD was higher than that of MFCs with 6.5 g/L COD, while the average removal rate of nitrate nitrogen of MFCs with 5 g/L COD was the lowest because of low COD concentration. The residual nitrate nitrogen concentration of MFCs with 11 g/L COD was 0 at the end of the 10th hour, while the residual nitrate nitrogen concentration of the other MFCs were basically 0 at the end of 11th hour, except for the MFCs with 5 g/L COD.

Changes of nitrite nitrogen (NO_2^--N) in electrolyte of MFCs was shown in Figure 2B. The nitrite nitrogen concentration gradually decreased from 4.2 to 0 mg/L within 4 h in MFC with COD concentration of 5 g/L. Nitrite nitrogen accumulation occurred in MFCs with COD concentrations of 6.5 g/L, 9.5 g/L and 11 g/L during the nitrate removal process, and the maximum nitrite nitrogen concentration of each group was 15.03 mg/L, 32.50 mg/L, 37.55 mg/L respectively at the end of the 4th hour. The accumulation of nitrite nitrogen was probably due to high ionic strength resulting from adding too much COD, which inhibited microbial metabolism. The higher the COD concentration was, the more significant the inhibition effect was, and the higher the nitrite nitrogen cumulative concentration was. At the same time, the accumulation of nitrite nitrogen might be the reason for the low average nitrate nitrogen removal rate during the 1st to the 4th hour. From the 5th to the 11th

hour, the nitrate removal rate decreased, i.e., the nitrite nitrogen generation rate decreased, and inhibition of microbial metabolism was gradually eliminated as COD concentration decreased, so the nitrite nitrogen concentration in MFCs gradually reduced to 0 when the COD concentration increased to over 6.5 g/L.

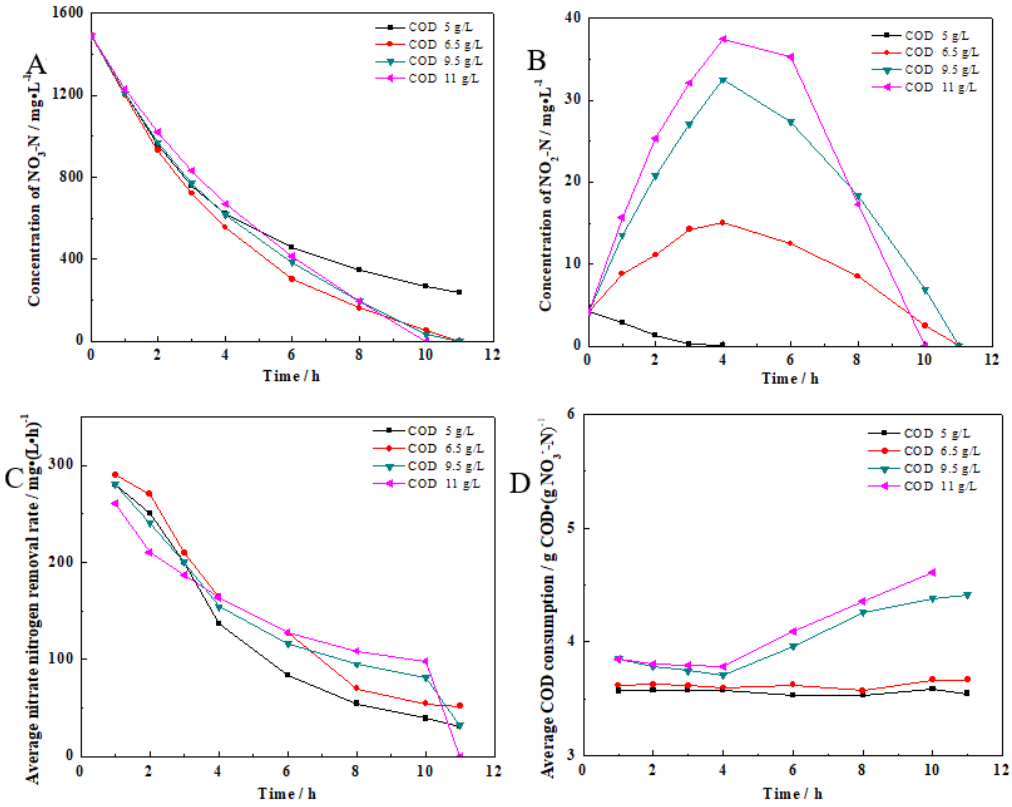


Figure 2. Changes of nitrate nitrogen concentration (**A**), nitrite nitrogen concentration (**B**), average nitrate nitrogen removal rate (**C**) and average COD consumption and COD (**D**) under different COD concentrations.

During the 1st to the 4th hour period, the average COD consumption for per nitrate nitrogen removal slightly decreased in MFCs as the COD concentration increased from 9.5 g/L to 11 g/L, because of incomplete reduction of nitrate. After the 4th hour, the average COD consumption increased along with the reduction of cumulative nitrite nitrogen. Among MFCs with COD concentrations of 5 g/L, the average COD consumptions per nitrate nitrogen removal were basically the same at every stage, and the values were higher than the theoretical value [56] because of consumption of non-denitrifying bacteria.

It can be seen from all of the above results that high COD concentration would lead to a decrease in nitrate nitrogen removal rate due to the inhabitation of microorganism metabolism and enzymatic activity, while insufficient COD concentration would cause nitrate incomplete reduction, resulting in the accumulation of harmful intermediate products [57]. The best nitrate removal effect was obtained at COD concentration of 6.5 g/L when using MFCs to treat this high nitrate content saline denitration solution.

3.1.2. Influence of COD Concentration on Electricity Generation

The output power density increased first, and then decreased as the COD concentration increased (Figure 3 Left). The highest maximum output power density was obtained at a COD concentration of 6.5 g/L, which was 231.2 mW/m^2 at a current density of 0.97 A/m^2, while the lowest maximum output power density was 135.2 mW/m^2 at a COD concentration of 5 g/L. Contrary to the change in output power density, the anodic potential decreased first, and then increased as COD concentration increased (Figure 3 Right). The anodic potential of MFCs at the COD concentration of 6.5 g/L was about 60 mV

lower than that at the COD concentration of 5 g/L. The difference in output power density might result from anodic potential since the cathodic polarization curves was almost the same, and the difference in anode potential might be caused by anodic pH because there was no buffer [58]. However, the maximum power density achieved in this study was lower than reported previously [51], which might be due to the pH and Ca^{2+}.

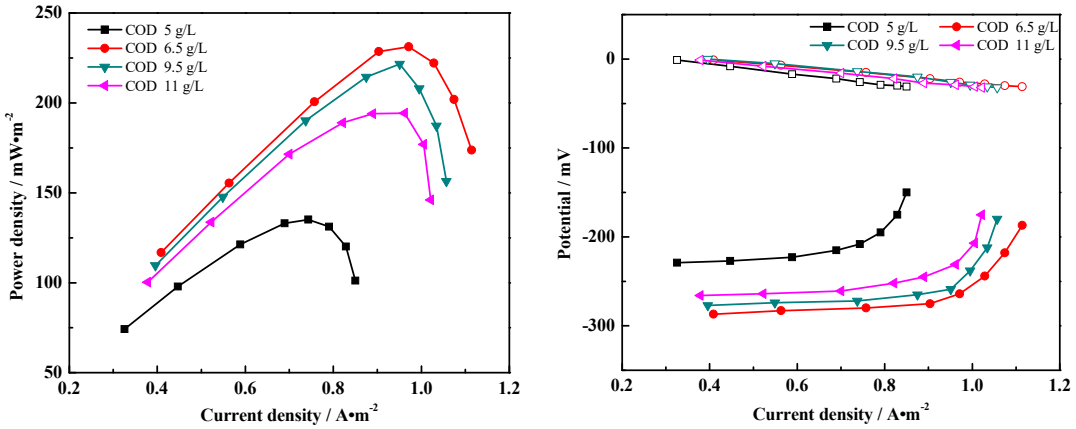


Figure 3. Power density curve (**Left**) and polarization curve ((**Right**): close circuit symbol, cathode potential; open circuit symbol, anode potential) under different COD concentrations.

On the one hand, OH^- was generated rapidly by reduction of nitrate at the anode during the denitrification process, which contributed to the rapid increase of the anodic pH (Figure S1). High anodic pH had an adverse effect on growth and metabolism of the microorganism, thus affecting the anodic reaction and anodic potential [59]. On the other hand, when 50 mM PBS was replaced with the denitration solution, PO_4^{3-} in residual solution on the surface of MFC anode was combined with Ca^{2+} in the denitration solution, forming $Ca_3(PO_4)_2$ precipitate and adhering to the surface of anode. Meanwhile, CO_2 from the oxidization of COD (NaAc) was dissolved into CO_3^{2-} at alkalinity, and then formed $CaCO_3$ precipitate. The loose and porous precipitate on the anodic surface ($Ca_3(PO_4)_2$ and $CaCO_3$ as shown in Figure S2) hindered mass transfer and reduced reactive sites, thus hindering the rate of the anodic reaction [60,61].

3.2. Influence of Initial Nitrate Nitrogen Concentration on Treatment of Saline Denitration Solution

3.2.1. Influence of Treatment Process on Removal of Nitrate Nitrogen

The evolution of nitrate nitrogen and nitrite nitrogen under different initial nitrate nitrogen concentrations during the denitrification process was shown in Figure 4. As the nitrate nitrogen concentration increased, the time required for complete removal of nitrate nitrogen increased. The average removal rate of nitrate nitrogen increased first and then decreased. It took 3 h to completely remove nitrate nitrogen in MFCs with initial nitrate nitrogen of 745 mg/L. The average removal rate was 248.3 mg/(L·h), which was the fastest among the group. The average nitrate nitrogen removal rates of MFCs with initial nitrate nitrogen of 1510 mg/L, 507 mg/L, 372 mg/L were 125.8 mg/(L·h), 169 mg/(L·h) and 124 mg/(L·h), respectively. In addition, the accumulation of nitrite nitrogen was observed in MFCs at the initial nitrate nitrogen concentration of 1510 mg/L during the denitrification process, and the accumulative concentration reached a peak of 37.5 mg/L at the 4th hour. Then, nitrite nitrogen gradually decreased to 0 at the 12th hour. The nitrite nitrogen concentration in the other groups was lower than 5 mg/L during the entire denitrification process.

There was no electricity generation from MFCs with an open circuit. One can note that the rate of nitrate nitrogen removal was significantly reduced under open-circuit conditions (Figure 4A). Using a conventional biological method to completely remove nitrate nitrogen with concentration of 745 mg/L took almost 24 h [41]. In our study, the

time taken for complete reduction of 745 mg/L nitrate nitrogen in MFCs at open-circuit was 12 h, while that at closed circuit was 3 h. Therefore, the average nitrate nitrogen removal rate at closed circuit was four-fold higher than that at the open-circuit and eight-fold higher than that of conventional biological method. In addition, under the circumstance of the same initial nitrate nitrogen concentration, MFCs with an open-circuit had a higher nitrite nitrogen accumulation than those with closed circuit. The maximum concentration of nitrite nitrogen accumulation in the denitrification process under the initial concentration of nitrate nitrogen of 1510 mg/L and open-circuit was up to 89.4 mg/L, which was more than twice as high as that at the closed circuit. This demonstrated that bioelectrochemical denitrification was significantly faster than the biological method. The difference between the average nitrate nitrogen removal rate of bioelectrochemical denitrification and the conventional biological method might result from accumulation of nitrite nitrogen. High nitrite nitrogen would form a high concentration of free nitrous acid (FNA) which causes inhibition for bacteria in wastewater treatment [58], while bioelectrochemical denitrification could effectively reduce accumulation of nitrite as well as FNA. Furthermore, the difference of nitrate removal performance between open-circuit and conventional biological way might result from a different microbial community since the electrochemistry in the process of MFCs start-up plays the role of selection.

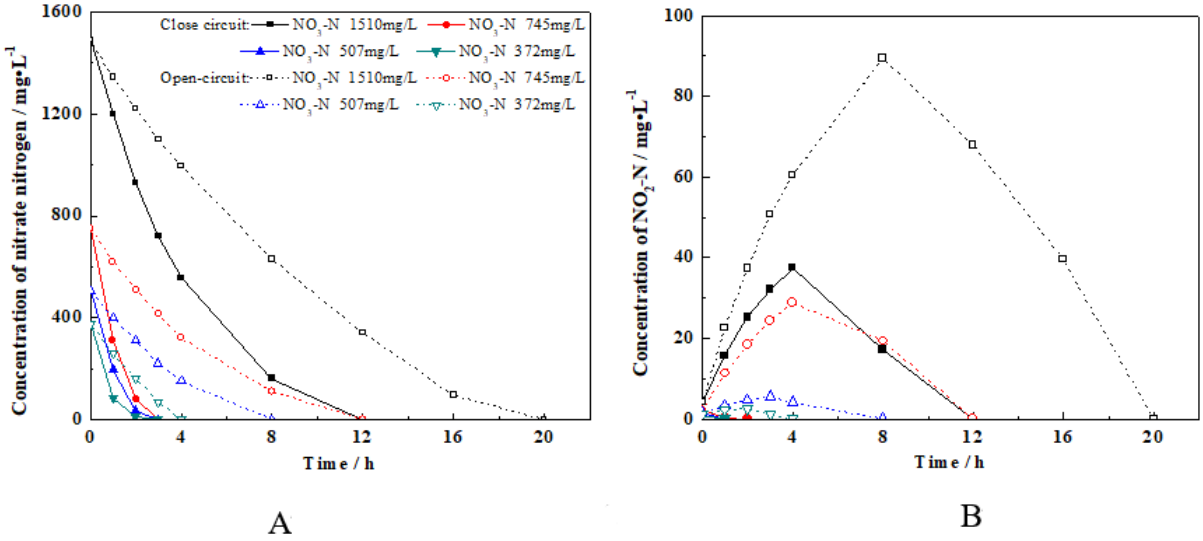


Figure 4. Changes of total nitrogen concentration (**A**) and nitrite nitrogen concentration (**B**) under open-circuit/closed-circuit.

After complete removal of nitrate nitrogen, some residual COD were observed in all MFCs. The average COD consumption per nitrate nitrogen removal during the whole process was 3.42 g, which was lower than most of the conventional biological methods [62]. This was probably because biological denitrification in MFC was essentially an anaerobic process [48] and certain non-exoelectrogenic bacteria activity was inhibited by high nitrate [52].

3.2.2. Influence of Initial Nitrate Nitrogen Concentration on Electricity Generation

The cathodic polarization curve of all MFCs were basically the same as shown in Figure 5, while the anodic potentials increased firstly and then decreased as the initial nitrate nitrogen concentration increase. The maximum output power density increased from 201.2 mW/m^2 to 241.1 mW/m^2 when the concentration of initial nitrate nitrogen increased from 372 mg/L to 745 mg/L, and then decreased to 231.2 mW/m^2 as initial nitrate nitrogen concentration increased to 1510 mg/L. Here, the anode potential shifted to more negative values as the initial nitrite concentration increased from 372 mg/L to 745 mg/L and then positively shifted a little bit as the initial nitrate nitrogen concentration

further increased to 1510 mg/L, while the cathode potential always kept an unchanged tendency, indicating that the increasing power density was mainly due to the enhancement in anode performance. The reason for the shift of the anode potential is not very clear, but we think it possibly relates to the pH change in the area around the anode. Because of the little buffering capacity of the saline denitration solution, the denitrification of nitrite released the OH^- and led to the pH increased in the area around the anode when the initial nitrite concentration was not high, resulting in the negative shift of anode potential. However, high pH could exhibit the activity of the bioanode, resulting in a little bit positive shift of anode potential [63] when the initial nitrite concentration further increased to 1510 mg/L.

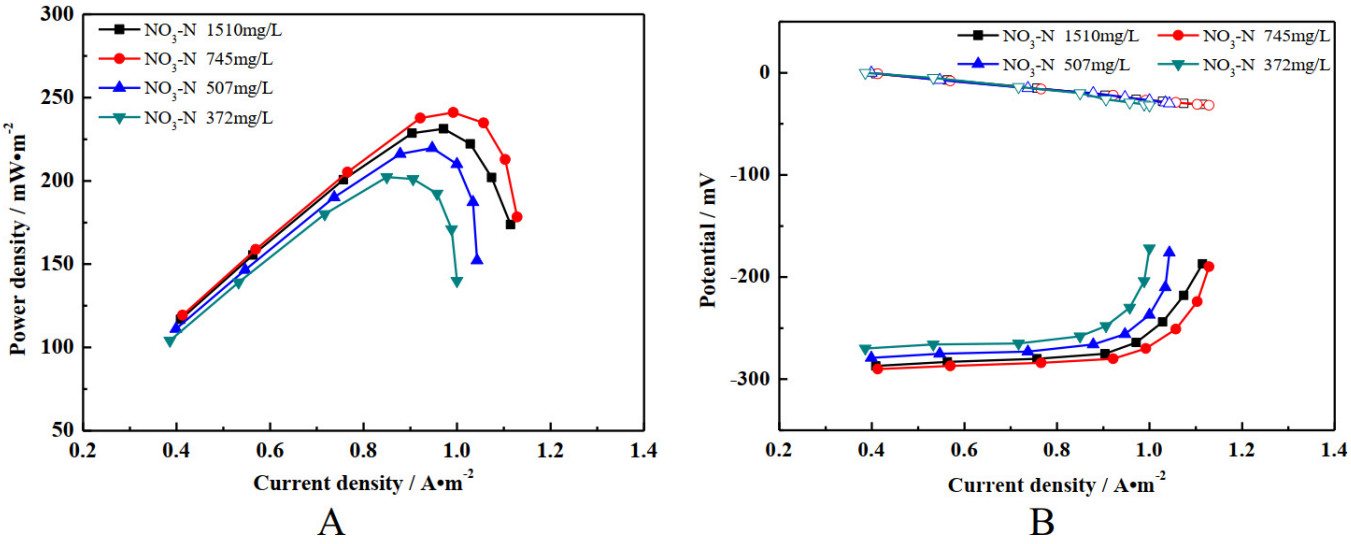


Figure 5. Power density curve (**A**) and polarization curve ((**B**): close circuit symbol, cathode potential; open circuit symbol, anode potential) under different initial nitrate nitrogen concentrations.

4. Conclusions

It is a difficult problem to efficiently treat saline wastewater with high nitrate content, The development of oxidation denitration technology is limited, even though it has high NO_X removal efficiency. Combined with MFC, ozone oxidation denitration can form a complete green process chain, and realize efficient and clean transformation of NO_X to N_2 in a coal-fired power plant. In the present study, ozone oxidation denitration solution with nitrate nitrogen of 1510 mg/L was treated by MFCs, and it could be completely removed within 10 h. When the initial nitrate nitrogen concentration was 745 mg/L and COD concentration was 6.5 g/L, the fastest average nitrate nitrogen removal rate was up to 248.3 mg/(L·h) which was eight fold higher than that of the conventional biological method, and the average COD consumption was 3.42 g/g-NO_3^--N which was lower than most conventional biological methods. Because of the influence of pH fluctuation and precipitate adhering at the anodic surface, the highest maximum output power density was only 241.1 mW/m^2.

Supplementary Materials: The following supporting information can be downloaded at: https://www.mdpi.com/article/10.3390/pr10081540/s1, Figure S1: Change of anodic pH at 6.5 g/L COD and 1510 mg/L NO_3^--N; Figure S2: XRD pattern of precipitate at anodic surface.

Author Contributions: Conceptualization, S.C. and Z.H.; methodology, validation, S.C., Z.H. and Z.W.; formal analysis, Z.H.; investigation, Z.H.; resources, S.C.; data curation, Z.H.; writing—original draft preparation, Z.H. and S.C.; writing—review and editing, S.C.; visualization, S.C. and Z.W.; supervision, S.C.; project administration, S.C. and Z.W.; funding acquisition, S.C. All authors have read and agreed to the published version of the manuscript.

Funding: This research was funded by the National Natural Science Foundation of China (No. 52070162).

Institutional Review Board Statement: Not applicable.

Informed Consent Statement: Not applicable.

Conflicts of Interest: The authors declare no conflict of interest.

References

1. Galloway, J.N. Acidification of the world: Natural and Anthropogenic. *Water Air Soil Pollut.* **2001**, *130*, 17–24. [CrossRef]
2. Niu, H.Y.; Leung, D.Y.C. A review on the removal of nitrogen oxides from polluted flow by bioreactors. *Environ. Rev.* **2010**, *18*, 175–189. [CrossRef]
3. Barman, S.; Philip, L. Integrated system for the treatment of oxides of nitrogen from flue gases. *Environ. Sci. Technol.* **2006**, *40*, 1035–1041. [CrossRef] [PubMed]
4. Wu, X.Q. Control measures of atmospheric nitrogen oxides pollution in China. *Environ. Prot.* **2009**, *426*, 9–11.
5. Zhang, Q.; Streets, D.G.; Carmichael, G.R.; He, K.B.; Huo, H.; Kannari, A.; Klimont, Z.; Park, I.S.; Reddy, S.; Fu, J.S.; et al. Asian emissions in 2006 for the NASA INTEX-B mission. *Atmos. Chem. Phys.* **2009**, *9*, 5131–5153. [CrossRef]
6. Wang, S.W.; Zhang, Q.; Streets, D.G.; He, K.B.; Martin, R.V.; Lamsal, L.N.; Chen, D.; Lei, Y.; Lu, Z. Growth in NO_X emissions from power plants in China: Bottom-up estimates and satellite observations. *Atmos. Chem. Phys.* **2012**, *12*, 4429–4447. [CrossRef]
7. Zheng, L.G.; Zhou, H.; Cen, K.F.; Wang, C.L. A comparative study of optimization algorithms for low NO_X combustion modification at a coal-fired utility boiler. *Expert Syst. Appl.* **2009**, *36*, 2780–2793. [CrossRef]
8. Spliethoff, H.; Greul, U.; Rüdiger, H.; Hein, K.R.G. Basic effects on NO_X emissions in air staging and reburning at a bench-scale test facility. *Fuel* **1996**, *75*, 560–564. [CrossRef]
9. Zhou, H.; Guo, X.T.; Zhou, M.X.; Ma, W.W.; Dahri, M.W.; Cen, K.F. Optimization of ammonia injection gridin hybrid selective non-catalyst reduction and selective catalyst reduction system to achieve ultra-low NOx emissions. *J. Energy Inst.* **2018**, *91*, 984–996. [CrossRef]
10. Liang, Z.Y.; Ma, X.Q.; Lin, H.; Tang, Y.T. The energy consumption and environmental impacts of SCR technology in China. *Appl. Energ.* **2011**, *88*, 1120–1129. [CrossRef]
11. Van Caneghem, J.; De Greef, J.; Block, C.; Vandecasteele, C. NOx reduction in waste incinerators by selective catalytic reduction(SCR) instead of selective noncatalytic reduction(SNCR) compared from a life cycle perspective: A case study. *J. Clean. Prod.* **2016**, *112*, 4452–4460. [CrossRef]
12. Mok, Y.S.; Ham, S.W. Conversion of NO to NO_2 in air by a pulsed corona discharge process. *Chem. Eng. Sci.* **1998**, *53*, 1667–1678. [CrossRef]
13. Chang, J.S.; Urashima, K.; Tong, Y.X.; Liu, W.P.; Wei, H.Y.; Yang, F.M.; Liu, X.J. Simultaneous removal of NO_X and SO_2 from coal boiler flue gases by DC corona discharge ammonia radical shower systems: Pilot plant tests. *J. Electrost.* **2003**, *57*, 313–323. [CrossRef]
14. Lin, H.; Gao, X.; Luo, Z.; Cen, K.F.; Huang, Z. Removal of NO_X with radical injection caused by corona discharge. *Fuel* **2004**, *83*, 1349–1355. [CrossRef]
15. Tsuji, K.; Shiraishi, I. Combined desulfurization/denitrification and reduction of air toxics using activated coke. *Fuel* **1997**, *76*, 549–559. [CrossRef]
16. Mochida, I.; Yozo, K. Removal of SO_2 and NO_X over activated carbon fibers. *Carbon* **2000**, *38*, 227–239. [CrossRef]
17. Gao, X.; Jiang, Y.; Zhong, Y.; Luo, Z.; Cen, K. The activity and characterization of CeO_2-TiO_2 catalysts prepared by the sol-gel method for selective catalytic reduction of NO with NH_3. *J. Hazard. Mater.* **2010**, *174*, 734–739. [CrossRef] [PubMed]
18. Kuehn, N.D. Retrofit control technology reducing NO_X emissions. *Power Eng.* **1994**, *98*, 23–27.
19. Forzatti, P. Present status and perspectives in de-NO_X SCR catalysis. *Appl. Catal. A Gen.* **2001**, *222*, 221–236. [CrossRef]
20. Jirat, J.; Stepanek, F.; Marek, M.; KubíEk, M. Comparison of design and operation strategies for temperature control during selective catalytic reduction of NO_X. *Chem. Eng. Technol.* **2001**, *24*, 35–40. [CrossRef]
21. Maisuls, S.E.; Seshan, K.; Feast, S.; Lercher, J.A. Selective catalytic reduction of NO_X to nitrogen over Co-Pt/ZSM-5 Part A. Characterization and kinetic studies. *Appl. Catal. B Environ.* **2001**, *29*, 69–81. [CrossRef]
22. Ergas, S.J.; Kinney, K.; Fuller, M.E.; Scow, K.M. Characterization of compost biofiltration system degrading dichloromethane. *Biotechnol. Bioeng.* **1994**, *44*, 1048–1054. [CrossRef] [PubMed]
23. Kennes, C.; Thalasso, F. Waste gas biotreatment technology. *J. Chem. Technol. Biotechnol.* **1998**, *72*, 303–319. [CrossRef]
24. Jin, Y.; Guo, L.; Veiga, M.C.; Kennes, C. Optimization of the treatment of carbon monoxide-polluted air in biofilters. *Chemosphere* **2009**, *74*, 332–337. [CrossRef] [PubMed]
25. Yang, W.F.; Hsing, H.J.; Yang, Y.C.; Shyng, J.Y. The effects of selected parameters on the nitric oxide removal by biofilter. *J. Hazard. Mater.* **2007**, *148*, 653–659. [CrossRef] [PubMed]
26. Zhu, H.S.; Mao, Y.P.; Yang, X.J.; Chen, Y.; Long, X.L.; Yuan, W.K. Simultaneous absorption of NO and SO_2 into Fe(II)–EDTA solution coupled with the Fe(II)–EDTA regeneration catalyzed by activated carbon. *Sep. Purif. Technol.* **2010**, *74*, 1–6. [CrossRef]

27. Chen, L.; Chung-Hao, H.; Yang, C. Oxidation and absorption of nitric oxide in a packed tower with sodium hypochlorite aqueous solutions. *Environ. Prog. Sustain. Energy* **2010**, *24*, 279–288. [CrossRef]
28. Hutson, N.D.; Krzyzynska, R.; Srivastava, R.K. Simultaneous removal of SO_2, NO_X, and Hg from coal flue gas using a $NaClO_2$-enhanced wet scrubber. *Ind. Eng. Chem. Res.* **2008**, *47*, 5825–5831. [CrossRef]
29. Guo, R.T.; Gao, X.; Pan, W.G.; Ren, J.X.; Wu, J.; Zhang, X.B. Absorption of NO into $NaClO_3$/NaOH solutions in a stirred tank reactor. *Fuel* **2010**, *89*, 3431–3435. [CrossRef]
30. Chu, H.; Chien, T.W.; Li, S.Y. Simultaneous absorption of SO_2 and NO from flue gas with $KMnO_4$/NaOH solutions. *Sci. Total Environ.* **2001**, *275*, 127–135. [CrossRef]
31. Wang, Z.H.; Zhou, J.H.; Zhu, Y.Q.; Wen, Z.; Liu, J.; Cen, K. Simultaneous removal of NO_X, SO_2 and Hg in nitrogen flow in a narrow reactor by ozone injection: Experimental results. *Fuel Processing Technol.* **2007**, *88*, 817–823. [CrossRef]
32. Wang, Z.H.; Zhou, J.H.; Fan, J.R.; Cen, K. Direct numerical simulation of ozone injection technology for NO_X control in flue gas. *Energy & Fuels* **2006**, *20*, 2432–2438.
33. Yoon, H.J.; Park, H.W.; Park, D.W. Simultaneous oxidation and absorption of NOx and SO_2 in an integrated O_3 oxidation/wet atomizing system. *Energy Fuels* **2016**, *30*, 3289–3297. [CrossRef]
34. Õgi, I.J.; Erme, K.; Raud, J.; Laan, M. Oxidation of NO by ozone in the presence of TiO_2 catalyst. *Fuel* **2016**, *173*, 45–51.
35. Lin, F.W.; Wang, Z.H.; Zhang, Z.M.; He, Y.; Zhu, Y.; Shao, J.; Yuan, D.; Chen, G.; Cen, K. Flue gas treatment with ozone oxidation: An overview on NOx, organic pollutants, and mercury. *Chem. Eng. J.* **2020**, *382*, 123030. [CrossRef]
36. Ono, Y.; Somiya, I.; Oda, Y. Identification of a carcinogenic heterocyclic amine in river water. *Water Res.* **2000**, *34*, 890–894. [CrossRef]
37. Jang, D.; Hwang, Y.; Shin, H.; Lee, W. Effects of salinity on the characteristics of biomass and membrane fouling in membrane bioreactors. *Bioresour. Technol.* **2013**, *141*, 50–56. [CrossRef]
38. Church, J.; Hwang, J.H.; Kim, K.T.; Mclean, R.; Oh, Y.K.; Nam, B.; Joo, J.C.; Lee, W.H. Effect of salt type and concentration on the growth and lipid content of *Chlorella vulgaris* in synthetic saline wastewater for biofuel production. *Bioresour. Technol.* **2017**, *243*, 147–153. [CrossRef]
39. Zhao, Y.; Feng, C.; Wang, Q.; Yang, Y.; Zhang, Z.; Sugiura, N. Nitrate removal from groundwater by cooperating heterotrophic with autotrophic denitrification in a biofilm-electrode reactor. *J. Hazard. Mater.* **2011**, *192*, 1033–1039. [CrossRef]
40. Tong, Y.; He, Z. Nitrate removal from groundwater driven by electricity generation and heterotrophic denitrification in a bioelectrochemical system. *J. Hazard. Mater.* **2013**, *262*, 614–619. [CrossRef]
41. Bilanovic, D.; Battistoni, P.; Cecchi, F.; Pavan, P.; Mata-Alvarez, J. Denitrification under high nitrate concentration and alternating anoxic conditions. *Water Res.* **1999**, *33*, 3311–3320. [CrossRef]
42. Fernándeznava, Y.; Marañón, E.; Soons, J.; Castrillón, L. Denitrification of high nitrate concentration wastewater using alternative carbon sources. *J. Hazard. Mater.* **2010**, *173*, 682–688. [CrossRef] [PubMed]
43. Dincer, A.R.; Kargi, F. Salt Inhibition of Nitrification and Denitrification in Saline Wastewater. *Environ. Technol. Lett.* **1999**, *20*, 1147–1153. [CrossRef]
44. Logan, B.E.; Hamelers, B.; Rozendal, R.; Schröder, U.; Keller, J.; Freguia, S.; Aelterman, P.; Verstraete, W.; Rabaey, K. Microbial fuel cells: Methodology and technology. *Environ. Sci. Technol.* **2006**, *40*, 5181–5192. [CrossRef]
45. Lovley, D.R. Bug juice: Harvesting electricity with microorganisms. *Nat. Rev. Microbiol.* **2006**, *4*, 497–508. [CrossRef]
46. Li, C.; Ren, H.Q.; Xu, M.; Cao, J. Study on anaerobic ammonium oxidation process coupled with denitrification microbial fuel cells (MFCs) and its microbial community analysis. *Bioresour. Technol.* **2015**, *175*, 545–552. [CrossRef]
47. Yuan, S.J.; Sheng, G.P.; Li, W.; Lin, Z.Q.; Zeng, R.J.; Tong, Z.H.; Yu, H.Q. Degradation of organic pollutants in a photoelectrocatalytic system enhanced by a microbial fuel cell. *Environ. Sci. Technol.* **2010**, *44*, 5575–5580. [CrossRef]
48. Tao, Q.; Luo, J.; Zhou, J.; Zhou, S.; Liu, G.; Zhang, R. Effect of dissolved oxygen on nitrogen and phosphorus removal and electricity production in microbial fuel cell. *Bioresour. Technol.* **2014**, *164*, 402–407. [CrossRef]
49. Allen, R.M.; Bennetto, H.P. Microbial fuel-cells. Electricity production from carbohydrates. *Appl. Biochem. Biotechnol.* **1993**, *39*, 27–40. [CrossRef]
50. Liu, J.; Wang, X.; Wang, Z.; Lu, Y.; Li, X.; Ren, Y. Integrating microbial fuel cells with anaerobic acidification and forward osmosis membrane for enhancing bio-electricity and water recovery from low-strength wastewater. *Water Res.* **2017**, *110*, 74–82. [CrossRef]
51. Zhang, J.; Zheng, P.; Zhang, M.; Chen, H.; Chen, T.; Xie, Z.; Cai, J. Kinetics of substrate removal and electricity generation in anodic denitrification microbial fuel cell (AD-MFC). *Bioresour. Technol.* **2013**, *149*, 44–50. [CrossRef] [PubMed]
52. Huang, H.; Cheng, S.; Yang, J.; Li, C.; Sun, Y.; Cen, K. Effect of nitrate on electricity generation in single-chamber air cathode microbial fuel cells. *Chem. Eng. J.* **2018**, *337*, 661–670. [CrossRef]
53. Cheng, S.; Wu, J. Air-cathode preparation with activated carbon as catalyst, PTFE as binder and nickel foam as current collector for microbial fuel cells. *Bioelectrochemistry* **2013**, *92*, 22–26. [CrossRef] [PubMed]
54. Jayashree, R.S.; Egas, D.; Spendelow, J.S.; Natarajan, D.; Markoski, L.J.; Kenis, P.J. Air-breathing laminar flow-based direct methanol fuel cell with alkaline electrolyte. *Electrochem. Solid-State Lett.* **2015**, *9*, 146–150. [CrossRef]
55. Gilcreas, F.W. Standard methods for the examination of water and waste water. *Am. J. Public Health Nations Health* **1966**, *56*, 387–388. [CrossRef]
56. McCarthy, P.L.; Beck, L.; Amant, P. Biological denitrification of wastewaters by addition of organic materials. In *Proceedings of the 24th Industrial Waste Conference*; Purdue University: West Lafayette, IN, USA, 1969; pp. 1271–1285.

57. Her, J.; Huang, J.S. Influences of carbon source and C/N ratio on nitrate/nitrite denitrification and carbon breakthrough. *Bioresour. Technol.* **1995**, *54*, 45–51. [CrossRef]
58. Zhou, Y.; Oehmen, A.; Lim, M.; Vadivelu, V.; Ng, W.J. The role of nitrite and free nitrous acid (FNA) in wastewater treatment plants. *Water Res.* **2011**, *45*, 4672–4682. [CrossRef]
59. Raghavulu, S.V.; Mohan, S.V.; Goud, R.K.; Sarma, P. Effect of anodic pH microenvironment on microbial fuel cell (MFC) performance in concurrence with aerated and ferricyanide catholytes. *Electrochem. Commun.* **2009**, *11*, 371–375. [CrossRef]
60. Jiang, D.; Curtis, M.; Troop, E.; Scheible, K.; Mcgrath, J.; Hu, B.; Suib, S.; Raymond, D.; Li, B. A pilot-scale study on utilizing multi-anode/cathode microbial fuel cells (MAC MFCs) to enhance the power production in wastewater treatment. *Int. J. Hydrogen Energy* **2011**, *36*, 876–884. [CrossRef]
61. Fernándeznava, Y.; Marañón, E.; Soons, J.; Castrillón, L. Denitrification of wastewater containing high nitrate and calcium concentrations. *Bioresour. Technol.* **2008**, *99*, 7976–7981. [CrossRef]
62. Henze, M. Capabilities of biological nitrogen removal process from wastewater. *Water Sci. Technol.* **1991**, *23*, 669–679. [CrossRef]
63. Fan, Y.; Hu, H.; Liu, H. Sustainable power generation in microbial fuel cells using bicarbonate buffer and proton transfer mechanisms. *Environ. Sci. Technol.* **2007**, *41*, 8154–8158. [CrossRef] [PubMed]